



Hydrothermal performance comparison of modified twisted tapes and wire coils in tubular heat exchanger using hybrid nanofluid

Sumit Kumar Singh, Jahar Sarkar *

Department of Mechanical Engineering, Indian Institute of Technology (BHU) Varanasi, UP, 221005, India

ARTICLE INFO

Keywords:

Tubular heat exchanger
Hybrid nanofluid
V-cuts twisted tape
Tapered wire coil
Hydrothermal performance
Performance evaluation criterion

ABSTRACT

A comparative experimental study to examine the hydrothermal behaviors of the double tube heat exchanger with various modified twisted tape and wire coil inserts is performed using Al_2O_3 +MWCNT hybrid nanofluid. The investigation is performed for Reynolds number of 8000–40000, nanofluid flow rate of 5–25 lpm and volume concentration of 0.01%. The effects of using various enhancers (V-cut twisted tapes and tapered wire coils) and hybrid nanofluid on the hydrothermal characteristics are assessed for different enhancer arrangements such as different twist ratios, V-cut depth ratios, V-cut width ratios, converging type (C-type) wire coil, diverging (D-type) wire coil and converging-diverging type (C-D type) wire coil. The test reveals that the pressure drop and heat transfer coefficient increase with reducing twist ratio, increasing depth ratio and reducing width ratio. D-type wire coil exhibits higher heat transfer performance with the penalty of pressure drop than that of other arrangements. V-cuts twisted tape of minimum twist ratio, maximum depth and width ratios yields maximum *PEC* and *FOM*. V-cut twisted tapes show a higher performance index than the tapered wire coil as the augmentation in pressure drop is slightly significant. D-type wire coil shows the minimum value of entropy generation among all other arrangements.

1. Introduction

Double tube heat exchangers are commonly used for the single-phase and phase change (condensing or evaporating) heat transfer in several applications in the power plant, chemical industry, waste heat recovery, refrigeration, automotive and process industries. Many efforts have been made to enhance the hydrothermal characteristics in double tube heat exchangers. There are numerous enhancement methods for improving the thermal performance of the double heat exchanger, namely active and passive methods. In the active method, it requires external power to enhance the heat transfer rate, such as surface vibrations, electrostatic fields, impinging jets, etc. Passive methods do not need any additional energy and have some other advantages, such as easy fabrication and low-cost implementation. Therefore, the passive method has become a promising method for heat exchangers [1]. The enhancers, which act as a passive method, are widely used in experimental as well as numerical investigations to examine the performance of the tubular heat exchangers [2–10]. Chamoli et al. [11,12] experimentally and numerically studied the thermal performance of circular tube fitted with novel type of perforated and anchor shaped vortex generators and found better

fluid mixing, which ultimately increases the heat transfer characteristics. Twisted tape (TT) and wire coil (WC) inserts as turbulators are some of the best methods that generate a swirl flow in the tube and diminishes the boundary layer thickness and consequently raise the turbulent intensity [13]. Also, the heat transfer rate of the heat exchanger may be improved by the use of heat transfer fluids of enhanced thermal conductivity. The stable nanofluids of low volume concentration of particles can provide remarkable improvement in the heat transfer properties. Nowadays, the hybrid nanofluids, which consist of the dispersion of two dissimilar nanoparticles in the base fluid, have been recently emerged as a next-generation working fluid to enhance the performance due to their enhanced thermophysical properties and slip mechanisms. Hence, in view of increased demand for energy density, the use of both enhancer (insert) and nanofluids can be a good combination to improve the heat transfer characteristics of the tubular heat exchanger.

Several investigators have been carried out on tubular heat exchanger by using both nanofluids and enhancers. Khoshvaght-Alabadi et al. [14] utilized spiky TT and water-based metallic nanofluids in the U-tube heat exchanger to investigate the hydrothermal characteristics and found that the spiky TT inserts of lower twist ratio and lower width/depth ratio using Ag/water nanofluid shows the maximum

* Corresponding author.

E-mail address: jsarkar.mec@itbhu.ac.in (J. Sarkar).

Abbreviations

DR	Depth ratio
FOM	Figure of merit
ID	Internal diameter
LMTD	Log mean temperature difference
MWCNT	Multi-walled carbon nanotube
OD	Outer diameter
PEC	Performance evaluation criterion
PI	Performance Index
TR	Twist ratio
TWC	Tapered wire coil
SEM	Scanning Electron Microscope
VCTT	V-cut twisted tape
WR	Width ratio

List of symbols

c_p	specific heat capacity [$\text{J}\cdot\text{kg}^{-1}\cdot\text{K}^{-1}$]
d	diameter [m]
D	width of the tape [m]
f	friction factor [–]
h	heat transfer coefficient [$\text{W}\cdot\text{K}^{-1}\cdot\text{m}^{-2}$]
H	pitch of the tape [m]
k	thermal conductivity [$\text{W}\cdot\text{K}^{-1}\cdot\text{m}^{-1}$]
Nu	Nusselt number [–]

m	mass flow rate [$\text{kg}\cdot\text{s}^{-1}$]
p	pressure [Pa]
Pe	depth of V-cut [m]
Pr	Prandtl number [–]
Q	heat transfer rate [W]
Re	Reynolds number [–]
S	entropy [$\text{W}\cdot\text{K}^{-1}$]
T	temperature [K]
\dot{V}	volume flow rate [lph]
w	width of V-cut [m]
W_p	Pumping power [W]

Greek symbols

Δ	drop
μ	dynamic viscosity [Pa.s]
ρ	density [$\text{kg}\cdot\text{m}^{-3}$]

Subscripts

bf	base fluid
gen	generation
h	hot fluid
nf	nanofluid
i, o	inner and outer
in, out	inlet and outlet
it, ot	inner tube and outer tube

augmentation of heat transfer coefficient. Akyurek et al. [15] used two wire coil turbulators of different pitches and alumina nanofluid and found that the Nusselt number and heat transfer coefficient enhanced by 180.47% and 14.21%, respectively, by using nanofluid. Reddy and Rao [16] found enhancement of 13.85% and 10.69% for heat transfer coefficient and friction factor with the combination of helical coil insert and TiO_2 nanofluid in the double tube heat exchanger. Mirzaei and Azimi [17] did an experimental study on hydrothermal characteristics with helical wire coil inserts using graphene oxide nanofluids and found 77% heat transfer coefficient augmentation. The heat transfer rate and pressure drop characteristics of a dimpled tube mounted with TT inserts using water-based TiO_2 nanofluid were determined by Eiamsa-ard et al. [18] and reported that the dimpled tube with higher dimple angle and lower twist ratio provides a higher heat transfer rate as well as pressure drop. He et al. [19] numerically investigated the performance of CuO nanofluid in a tube with single and double twisted tapes and found that a tube with a single TT has a higher value of PEC than that of the tube with two TTs, which indicates that using a tube with a single TT is satisfactory from a fluid-thermal viewpoint. Bazdidi-Tehrani et al. [20] numerically studied the heat transfer behavior of CMC/CuO nanofluid with the use of TT inserts and found an enhancement of 60% and 22.2% for Nusselt number and friction factor at 1.5% particle concentration and the twist ratio of 5, respectively. Naik et al. [21] used both TT inserts and WC insert and observed that WC inserts provide better heat transfer performance using CuO nanofluid. Akhavan-Behabadi et al. [22] found the thermal performance factor greater than one with WC inserts in a tube using MWCNT nanofluid. Few researchers have carried out studies with hybrid nanofluids. Singh and Sarkar [23] used $\text{Al}_2\text{O}_3+\text{TiO}_2$ water-based hybrid nanofluid and V-cut twisted tape (VCTT) inserts to investigate the thermal-hydraulics performance and observed that Nusselt number and friction factor increases with lowering the twist ratio, rising the V-cut depth ratio and reducing the V-cut width ratio. Maddah et al. [24] observed the advantages of TT inserts and $\text{Al}_2\text{O}_3+\text{TiO}_2$ hybrid nanofluid in exergetic performance. They concluded that the combination of twisted tape and hybrid nanofluid led to an increase in the exergy efficiency in comparison to the base fluid. Recently, Singh and Sarkar [25] used PCM dispersed mono/hybrid nanofluids in a concentric tube heat

exchanger with a VCTT turbulator and reported that PCM nanofluid shows the maximum value of heat transfer coefficient to pressure drop ratio at a lower flow rate. Bahiraei et al. [26] analyzed the irreversibility of GNP hybrid nanofluid in a tube with a double TT insert and observed more irreversibility reduction for double counter TT inserts. Singh and Sarkar [27] used a novel tapered wire coil inserts in a tubular heat exchanger using $\text{Al}_2\text{O}_3+\text{MgO}$ hybrid nanofluid and observed that diverging type tapered coil promotes better heat transfer. Li et al. [28] studied the effects of CuO nanofluid and fin geometries on boiling heat transfer and found the reduction in fouling with the modified surface and higher heat transfer coefficient with higher height and lower width of the fins. Moreover, Li et al. [29] studied the boiling heat transfer of CuO-water over a transient study and identified that the heat transfer coefficient was suppressed due to the development of the fouling layer over 1000 min of continuous measurement.

However, based on the literature review, few experimental studies have been conducted so far for both hybrid nanofluid and enhancer (modified twisted tape or modified wire coil). As far as the authors know, none of the studies deals with the comparison of V-cut twisted tape and tapered wire coil insertions using hybrid nanofluid as a coolant. Moreover, no study is available, which mentions the performance characteristics parameters such as performance evaluation criterion, figure of merit and performance index of the double tube heat exchanger with various enhancers using hybrid nanofluids.

Hence, to fulfill the above research gap, the improvements of hydrothermal characteristics of the double tube heat exchanger with the various enhancers (V-cut twisted tape and tapered wire coil) using water-based $\text{Al}_2\text{O}_3+\text{MWCNT}$ hybrid nanofluids are experimentally compared. The experiments were performed for different V-cut twisted tapes, wire coil arrangements, nanofluid flow rate and Reynolds number. In addition, the impact of various enhancers and hybrid nanofluids on the various hydrothermal performance parameters such as performance evaluation criterion (PEC), figure of merit (FOM) and performance index (PI) are discussed. The impact on the entropy generation is investigated as well. This comparative study of the tubular heat exchanger with various enhancers (modified twisted tapes and modified wire coils) will be useful for researchers in the research area related to

the application of a different class of tube inserts in order to understand the prevailing mechanism of fluid flow and heat transfer and also will bring more development in tubular heat exchanger systems.

2. Methodology

2.1. Hybrid nanofluid synthesis and characterization

In this study, the hybrid nanofluid was synthesized by mixing Al_2O_3 and MWCNT nanoparticles (have been chosen due to their low cost, easy availability and considerable thermal conductivity values) with an equal volume ratio in DI water for 0.01% total volume concentration. The properties of Al_2O_3 and MWCNT particles have been taken from the previous study [30]. Table 1 shows the properties of the base fluid, nanoparticles (Al_2O_3 , MWCNT) and hybrid nanofluid (Al_2O_3 +MWCNT) at ambient temperature. After dispersing nanoparticles in DI water, it was sonicated for 3 h using an ultrasonic vibration bath to avoid the sedimentation of the nanofluid. Fig. 1(a) shows the images of Al_2O_3 +MWCNT hybrid nanofluid obtained from the SEM test and exposes that Al_2O_3 nanoparticles are in a spherical shape of diameter varying between 10 and 100 nm and MWCNT particles are in a cylindrical shape. Additionally, the prepared hybrid nanofluid was characterized by X-ray diffractometer, as shown in Fig. 1(b). The MWCNT displays peak pattern at 26.2, 42.98, 54.89 and 77.94 corresponding to [003], [102], [005] and [1050] diffracted planes, respectively. Also, the highest peaks of Al_2O_3 +MWCNT were noticed in XRD at 41.8°, 52.32° and 74.89°, corresponding to [112], [180], and [200] planes, respectively. Therefore, the XRD investigation ensured that the Al_2O_3 and MWCNT nanoparticles were successfully suspended in a base fluid. The visual observation of hybrid nanofluid was done to examine the stability as shown in Fig. 2 and found that the hybrid nanofluid had sufficient stability (up to 10 days). Moreover, the pH value of synthesized hybrid nanofluid was measured to check the stability. Its value was found far away from the nanoparticle's isoelectric point (IEP), i.e., the pH value at which the nanoparticle does not carry any net electrical charge. The pH value of Al_2O_3 +MWCNT of 0.01 vol% is 7.73 and the IEP of Al_2O_3 and MWCNT are 9.1 and 4.5, respectively, which is far away from its pH value [31,32].

The thermal property analyzer (Hot disk TPS-500) with an accuracy of $\pm 1\%$ was used to evaluate the specific heat and thermal conductivity of the prepared nanofluid. The dynamic viscosity of hybrid nanofluid was measured by a digital viscometer (LVDV-II + Pro Brookfield). For the density of hybrid nanofluid, the known volume of nanofluid was taken in a measuring beaker and weighted in digital weighing balance (model: ATX224, Shimadzu, Japan). From the obtained weight, the weight of the empty measuring beaker was subtracted to get the weight of the nanofluid. The prepared nanofluid density was estimated by dividing this weight by the known volume of the nanofluid.

2.2. Test facility and method

The schematic outline and the photograph of the test setup, mainly consisting of the test section (double tube heat exchanger with the inner tube of $ID = 18$ mm and $OD = 26$ mm) and flow loops, are shown in Fig. 3 (a) and (b). The inlet temperature of hot fluid was adjusted by an electric heater attached to the heating tank with a temperature

controller. The chiller, attached with a cold tank, was used for cooling the warm fluid. Two centrifugal pumps were used to drive both fluids in the heat exchanger. With the help of centrifugal pumps, hybrid nanofluid was pumped through the inner tube, whereas DI water as a hot fluid was passed through the outer tube of internal diameter 47 mm in the opposite direction. The asbestos rope was mounted over the test section to decrease the heat losses to the environment. To measure the fluid temperatures, four different PT-100 thermometers were used. The flow rates of the fluids were measured by using rotameters installed in each loop with control valves. The measurement of pressure drop in the inner tube and annulus was carried out by the U-tube manometer. The temperature of hybrid nanofluid in the cold tank was maintained at 30 °C by adjusting with the chiller unit and flow rate ranging from 5 to 25 lpm. The hot fluid was flowing in the annulus at a uniform temperature of 60 °C with a constant flow rate of 15 lpm. After reaching a steady-state for each test run, the temperatures and pressure drops were recorded.

The image of V-cut twisted tapes (VCTT) and tapered wire coil (TWC) with different configurations are shown in Fig. 4. However, the major criteria for choosing the size and arrangement of the VCTT and TWC is the high value of the thermal performance factor. All the dimensions of the V-cut in the VCTT and arrangements of TWC are selected as per the requirement depending on the size of the tapes, wire coil and inner tube. Aluminium strips with V-cuts were twisted uniformly along their length to get the V-cuts twisted tapes (VCTT) with different twist ratios, whereas the tapered wire coils were fabricated with a uniform pitch. VCTT of various twist ratios ($TR = H/D$) of 5, 10 and 15, depth ratios ($DR = Pe/D$) of 0.33 and 0.5 and width ratios ($WR = w/D$) of 0.33 and 0.5 and TWC of diverging (D), converging (C) and converging-diverging (C-D) types were used as an enhancer. Detailed dimensions of enhancers (VCTT and TWC) are summarized in Table 2.

2.3. Post-processing

The heat gain by cold fluid and that supplied by the hot fluid are determined by,

$$Q_{nf} = \dot{V}_{nf} \rho_{nf} c_{p,nf} (T_{nf,out} - T_{nf,in}) \quad (1)$$

$$Q_h = \dot{V}_h \rho_h c_{p,h} (T_{h,in} - T_{h,out}) \quad (2)$$

The mean heat transfer rate is measured by,

$$Q_{avg} = (Q_{nf} + Q_h) / 2 \quad (3)$$

Equation (4) is used to estimate the overall heat transfer coefficient,

$$U_{in} = \frac{Q_{avg}}{A_{in} \times \Delta T_{LMTD}} = \frac{(T_{h,in} - T_{nf,out}) - (T_{h,out} - T_{nf,in})}{\ln \left(\frac{T_{h,in} - T_{nf,out}}{T_{h,out} - T_{nf,in}} \right)} \quad (4)$$

Heat transfer coefficient (hybrid nanofluid) without considering fouling can be estimated by,

$$\frac{1}{U_{in} A_{in}} = \frac{1}{h_{nf} A_{in}} + \frac{\ln \left(\frac{d_o}{d_i} \right)}{2\pi k L} + \frac{1}{h_{out} A_{out}} \quad (5)$$

Nusselt number of outer tube is calculated by using correlation [33],

Table 1

Thermo-physical properties of base fluid, nanoparticles and hybrid nanofluid.

Materials	Thermal conductivity (W/m.K)	Density (kg/m ³)	Specific heat (J/kg.K)	Viscosity (Pa.s)	pH Value
Water	0.6014	995	4183	0.0007623	6.96
Al_2O_3 [30]	40	3900	880	–	–
MWCNT [30]	3000	2660	740	–	–
Al_2O_3 + MWCNT (nanofluid)	0.6061	995.8	4181	0.0007996	7.73

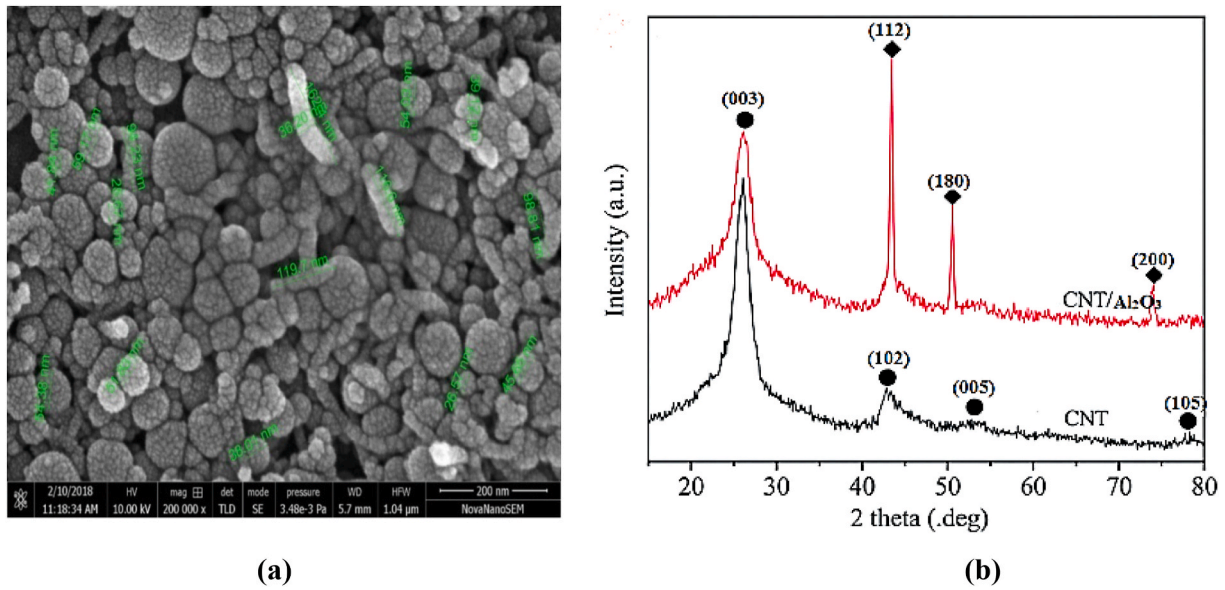
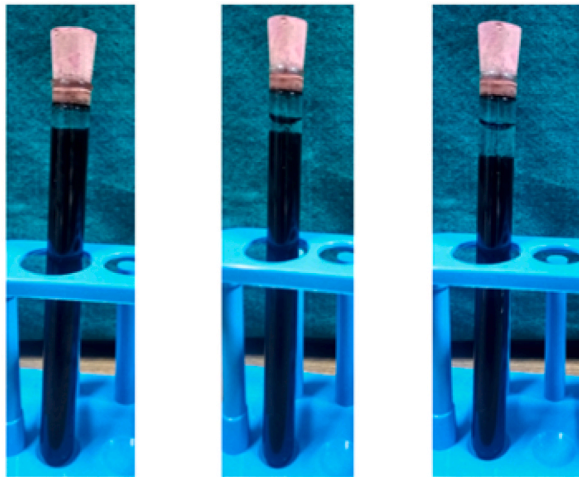


Fig. 1. (a) SEM and (b) XRD image of Al_2O_3 +MWCNT hybrid nanofluid.



After preparation After 5 days After 10 days

Fig. 2. Sedimentation observation of Al_2O_3 +MWCNT (0.01 vol %) hybrid nanofluid.

$$Nu_{out} = 0.007435Re^{0.91}Pr^{1/3}\left(\frac{\mu}{\mu_w}\right)^{0.14} \quad (6)$$

Range: $4000 < Re < 30000$, $1.72 < d_{ob,i}/d_{ib,o} < 3.2$.

Annulus side heat transfer coefficient has been estimated by,

$$h_{out} = \frac{Nu_{out} \times k_{nf}}{d_{eqv}} \quad (7)$$

where d_{eqv} is given by, $d_{eqv} = (d_{it,o}^2 - d_{it,i}^2)/d_{it,o}$

From equations (7) and (5), the Nusselt number of nanofluid is expressed as follows:

$$Nu_{nf} = h_{nf}d_{it,i}/k_{nf} \quad (8)$$

The expression for the friction factor is given below;

$$f = \frac{\pi^2}{8} \Delta p \left(\frac{\rho_{nf}d_{it,i}^5}{\dot{m}_{nf}^2 L} \right) \quad (9)$$

Pumping power is determined by,

$$W_p = \dot{V}\Delta p \quad (10)$$

The performance evaluation criterion (PEC) is calculated by,

$$PEC = \frac{Nu_{nf}}{Nu_{bf}} \left/ \left(\frac{f_{nf}}{f_{bf}} \right)^{1/5} \right. \quad (11)$$

The figure of merit (FOM) is estimated by,

$$FOM = \frac{h_{nf}}{h_{bf}} \left/ \left(\frac{W_{pnf}}{W_{pbf}} \right)^{1/5} \right. \quad (12)$$

Performance index (PI) is determined by,

$$PI = \frac{Q}{W_p} \quad (13)$$

There are two types of irreversibilities present in the heat exchanger, caused by heat transfer and fluid friction. The rate of total entropy generation within the heat exchanger is determined by applying the entropy balance on the entire heat exchanger.

Total entropy generation can be determined as follow;

$$S_{gen,tot} = S_{gen,th} + S_{gen,f} \quad (14)$$

where,

$$S_{gen,th} = m_{nf}c_{p,nf} \ln\left(\frac{T_{nf,out}}{T_{nf,in}}\right) + m_h c_{p,h} \ln\left(\frac{T_{h,out}}{T_{h,in}}\right) \quad (15)$$

$$S_{gen,f} = \frac{m_{nf} \times \Delta p_c}{\rho_{nf} \times T_{avg,c}} + \frac{m_h \times \Delta p_h}{\rho_h \times T_{avg,h}} \quad (16)$$

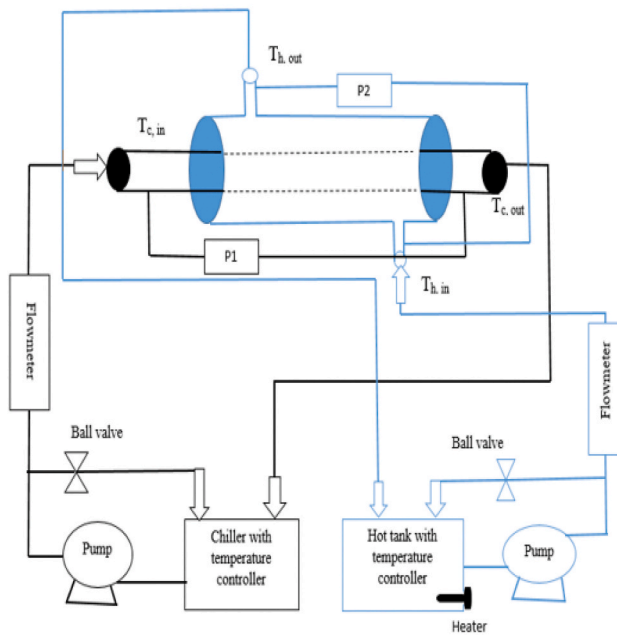
Therefore, total entropy generation can be written as;

$$S_{gen,tot} = m_{nf}c_{p,nf} \ln\left(\frac{T_{nf,out}}{T_{nf,in}}\right) + \frac{m_{nf} \times \Delta p_c}{\rho_{nf} \times T_{avg,c}} + m_h c_{p,h} \ln\left(\frac{T_{h,out}}{T_{h,in}}\right) + \frac{m_h \times \Delta p_h}{\rho_h \times T_{avg,h}} \quad (17)$$

Also, the entropy rises in the tube carrying nanofluid is evaluated by,

$$\Delta S_{nf} = m_{nf}c_{p,nf} \ln\left(\frac{T_{nf,out}}{T_{nf,in}}\right) + \frac{m_{nf} \times \Delta p_c}{\rho_{nf} \times T_{avg,c}} \quad (18)$$

The most commonly used dimensionless form, called the entropy



(a)

(b)

Fig. 3. (a) Layout of the experimental setup (b) Photograph of the experimental setup.

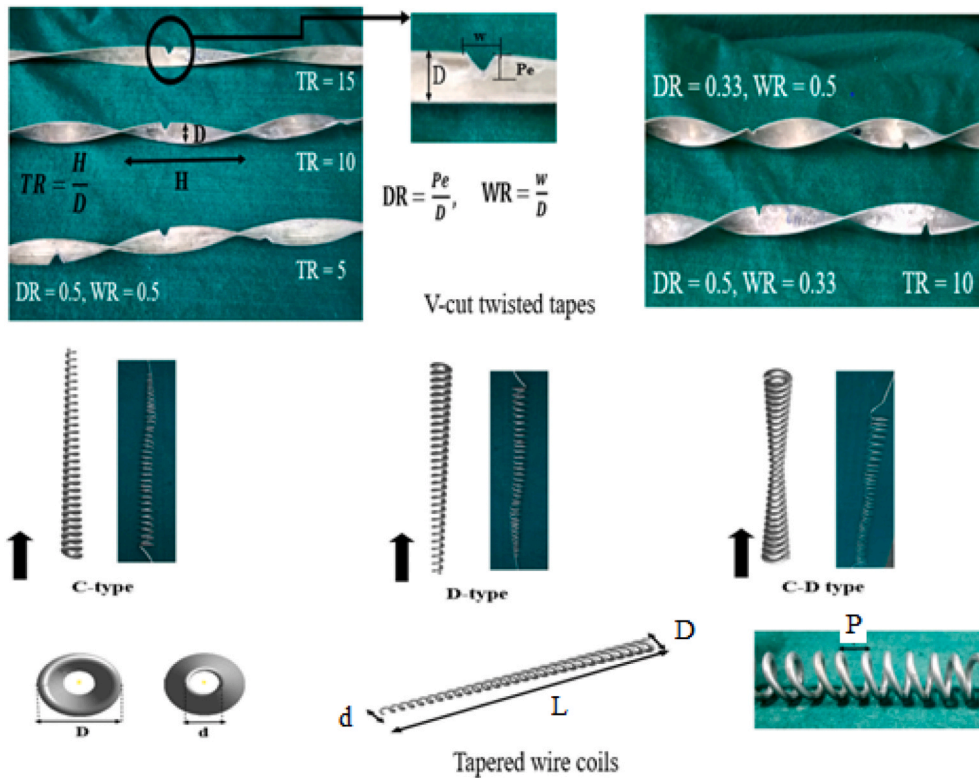


Fig. 4. Photograph of various twisted tape and wire coil inserts.

generation number is defined as;

$$N_s = \frac{S_{gen}}{(\dot{m}c_p)_{min}} \tag{19}$$

where the denominator represents the fluid of minimum heat capacity rate.

To estimate the contribution of each irreversibility, the dimensionless parameter, Bejan number is defined as the ratio of entropy generation due to heat transfer rate to the total entropy generation rate, as

Table 2
Details of enhancers and its geometry.

Parameter	Value
Tape width (D)	15 mm
Tape thickness	1 mm
Twist ratio (TR = H/D)	5, 10 and 15
Depth of the V-cuts (P _e)	5 and 7.5 mm
Width of the V-cuts (w)	5 and 7.5 mm
Depth ratio (DR = P _e /D)	0.5 and 0.33
Width ratio (WR = w/D)	0.5 and 0.33
Wire diameter	2 mm
Pitch of the tapered wire coil, P	10 mm
Larger end diameter of tapered wire coil, D	13 mm
Smaller end diameter of tapered wire coil, d	6.5 mm

given below:

$$Be = \frac{S_{gen,th}}{S_{gen,tot}} \quad (20)$$

2.4. Uncertainty analysis

By taking the relative error of independent parameters (x_n) such as temperature (T), volume flow rate (V̇) and pressure drop (Δp), the uncertainty analysis of dependent parameters (X) can be computed by using equations developed by Kline and McClintock [34],

$$\frac{\delta X}{X} = \sqrt{\left(\frac{\delta x_1}{x_1}\right)^2 + \left(\frac{\delta x_2}{x_2}\right)^2 + \dots + \left(\frac{\delta x_n}{x_n}\right)^2} \quad (21)$$

The uncertainties value of independent parameters such as T, V̇ and Δp are ±0.33 °C, ±0.714% and ±2.58%, respectively. The uncertainty values of estimated parameters are presented in Table 3.

2.5. Validation of plain tube with DI water

To ensure the accuracy of experimental data, the experiment was carried out on a tube without insert using water and the results obtained were compared with Sieder and Tate [35] correlation (Eq. (22)) and Nanan et al. [36] correlation (Eqs. (23) and (24)) for Nusselt number and friction factor as shown in Fig. 5, respectively.

$$Nu = 0.027Re^{0.8}Pr^{0.33}\left(\frac{\mu}{\mu_s}\right)^{0.14} \quad (22)$$

$$Nu = 0.0068Re^{0.92}Pr^{0.4} \quad (23)$$

$$f = 1.01Re^{-0.37} \quad (24)$$

From the figure, it is concluded that the experimental data are in acceptable range with the Sieder-Tate and Nanan et al. correlations for Nusselt number with a mean deviation of ±12.9% and ±9.5%, respectively, while the friction factor is agreed well with the Nanan et al. correlation with an average deviation of ±6.4%.

Table 3
Uncertainty of parameters.

Parameter	Uncertainty (%)
Temperature, T	±0.33
Density, ρ	±1
Viscosity, μ	±1
Thermal conductivity, k	±1
Reynolds number, Re	±1.22
Heat transfer rate, Q	±1.27
Overall heat transfer coefficient, U	±1.31
Heat transfer coefficient, h	±2.13
Nusselt number, Nu	±2.35
Friction factor, f	±6.45
Entropy generation, S _{gen}	±6.10

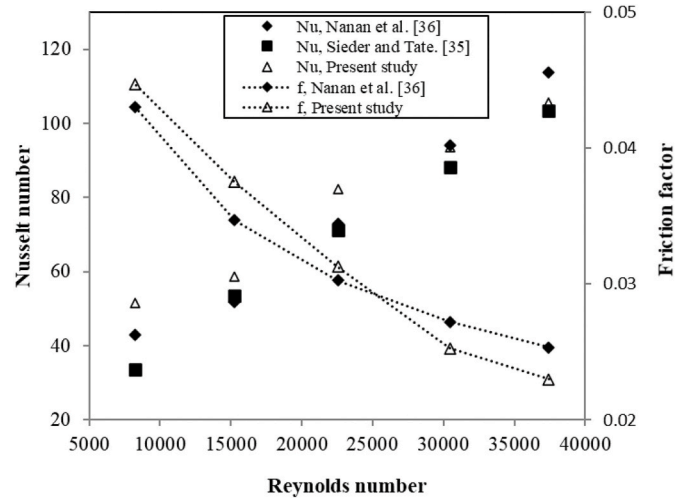


Fig. 5. Validation of Nusselt number and friction factor for water in a plain tube.

3. Results and discussion

3.1. Heat transfer and pressure drop

The effects of enhancers (V-cut twisted tapes and tapered wire coils) with different arrangements on the heat transfer coefficient (h_{nf}) are shown in Fig. 6. It is clear from the figures that the significant increase in h_{nf} with an increase in nanofluid flow rate is obtained by inserting the enhancers. The heat transfer coefficient is a quantitative characteristic of convection between a fluid and surface wall. It depends on transport properties of fluid, nature of fluid flow and hydrodynamic and thermal boundary conditions. While Nusselt number is the augmentation of heat transfer due to convection over the conduction. The h_{nf} is attained higher with tapered wire coil than V-cut twisted tapes. The reason is that the boundary layer thickness weakens by inserting a tapered wire coil, which raises the swirl flow at a different radial distance in the tube and promotes better heat transfer. It is clear that the augmentation in heat transfer is mainly caused by the change in flow pattern near the wall surface. The implementation of tapered wire coil inserts induces the separated flow along with the secondary flow over the wire coil. The

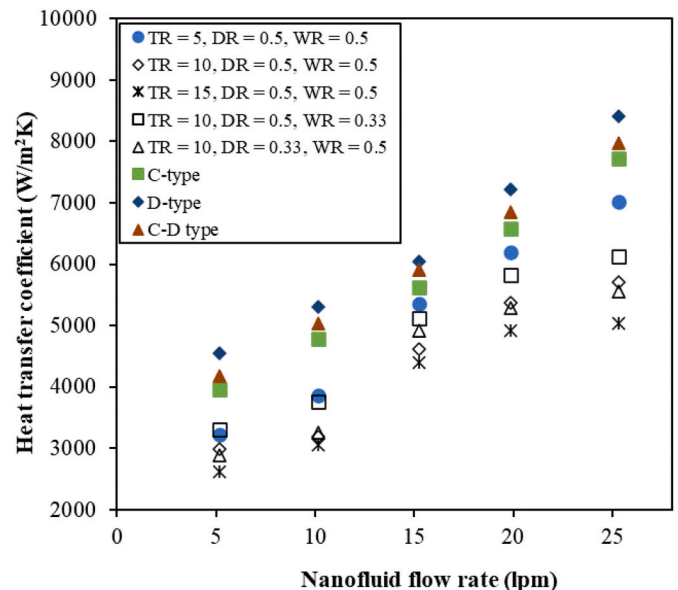


Fig. 6. Variation of heat transfer coefficient with nanofluid flow rate.

coaction of secondary flow and separated main flow exhibit significant heat transfer augmentation [37]. While the insertion of V-cut twisted tape in a tube, the vorticity behind the cuts offers extra turbulence near the tube wall. The interaction of vortex circulation, together with secondary flow, increases the turbulence near the heated surface of the tube. Also, the thermal conductivity of MWCNT nanoparticles is higher than that of DI water, which leads to improving heat transfer. D-type wire coil exhibits higher heat transfer performance than other enhancers due to an increase in residence time of flow and contact surface area when the fluid slowdown from diverging wire coil. The maximum value of h_{nf} correspond to D-type wire coil, i.e., 8411.46 W/m²K while the minimum value of h_{nf} correspond to VCTT of $TR = 15$, $DR = 0.5$ and $WR = 0.5$, i.e., 5036.43 W/m²K at a high nanofluid flow rate (25 lpm), respectively. Among the tapered wire coil insert arrangements, the h_{nf} is attained maximum values with D-type wire coil followed by C-D type wire coil (7978.03 W/m²K) and C-type wire (7726.38 W/m²K), respectively, at a high nanofluid flow rate (25 lpm). In the case of using VCTT, it is noticeable that the heat transfer characteristic is enhanced by decreasing the twist ratio (TR), raising the depth ratio (DR) and reducing the width ratio (WR). For the same $DR = 0.5$ and $WR = 0.5$, the h_{nf} is attained maximum value with V-cut twisted tape of $TR = 5$, i.e., 7020.18 W/m²K followed by with $TR = 10$ (5709.59 W/m²K) and $TR = 15$ (5036.43 W/m²K) at a high nanofluid flow rate (25 lpm), respectively. Similarly, for the same $TR = 10$, the h_{nf} is attained maximum values with VCTT of depth ratio of 0.5 and width ratio of 0.33, i.e., 6125.40 W/m²K than with VCTT of depth ratio of 0.33 and width ratio of 0.5 (5549 W/m²K). In comparison to DI water in a smooth tube, the h_{nf} is attained the average enhancements of 142.41% and 99.13%, with D-type wire coil and VCTT of $TR = 5$, $DR = 0.5$ and $WR = 0.5$, respectively.

Fig. 7 illustrates the comparison of pressure drop (Δp) of Al₂O₃+MWCNT hybrid nanofluid for different arrangements of enhancers. It is evident from the figures that while increasing the nanofluid flow rate, the Δp increases with the rise in nanofluid flow rate. When the fluid flows through the tube, the friction causes the pressure drop. The Δp and f are higher by using tapered wire coils as compared to that by using V-cut twisted tapes. Also, the Δp and f increase due to the effect of enhancement in viscosity of the Al₂O₃+MWCNT hybrid nanofluid. The diverging wire coil shows a higher Δp than that of the other arrangements due to the disturbing of the flow at the entrance of diverging wire coil inserts and leads to an increase in the Δp . The outcomes expose that the Δp rises with decreasing the twist ratio, raising the DR and reducing the WR . At the same nanofluid flow rate (25 lpm), the maximum value of

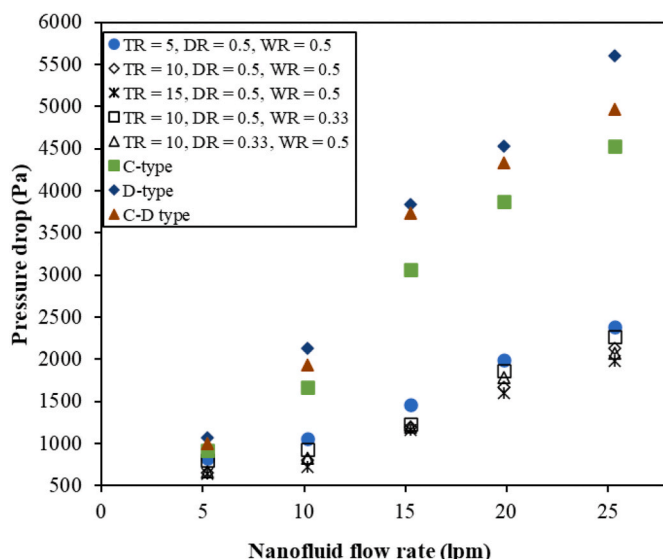


Fig. 7. Variation of pressure drop with nanofluid flow rate.

Δp corresponds to D-type wire coil, i.e., 5603.47 Pa, while the minimum value of Δp corresponds to VCTT of $TR = 15$, $DR = 0.5$ and $WR = 0.5$, i.e., 1974.55 Pa. For the same depth ratio (0.5) and width ratio (0.5), the Δp is attained maximum value with VCTT of $TR = 5$, i.e., 2388.02 Pa, followed by with $TR = 10$ (2134.65 Pa) and $TR = 15$ (1974.55 Pa) at the nanofluid flow rate of 25 lpm, respectively. Likewise, for the same $TR = 10$, the Δp is attained maximum value with VCTT of depth ratio of 0.5 and width ratio of 0.33, i.e., 2264 Pa than with VCTT of depth ratio of 0.33 and width ratio of 0.5 (2054.65 Pa), respectively. In comparison to DI water in a plain tube, the Δp is attained the average enhancement of 547.85% and 218.46% with D-type wire coil and VCTT of $TR = 5$, $DR = 0.5$ and $WR = 0.5$, respectively.

3.2. Nusselt number and friction factor

The variation of Nusselt number enhancement ratio (Nu_{insert}/Nu_{plane}) and friction factor ratio (f_{insert}/f_{plain}) with respect to Reynolds number for different arrangements of the enhancer is shown in Figs. 8 and 9. The result reveals that the Nusselt number enhancement ratio first increases up to the Reynolds number of 15,000 and then decreases with the Reynolds number. The ratio is attained higher with tapered wire coil than V-cut twisted tapes. D-type wire coil shows a maximum value of Nu_{insert}/Nu_{plane} among all arrangements of enhancers. Also, it is observed that the values of the ratio are greater than unity for all cases, which implies a useful advantage for heat transfer enhancement using all enhancers over the plane tube. The range of Nu_{insert}/Nu_{plane} is around 1.93–2.68 for tapered wire coil and 1.40–2.18 for V-cut twisted tapes inserts. The value of the ratio (Nu_{insert}/Nu_{plane}) ranges from 2.28 to 2.68 for D-type wire coil, from 2.02 to 2.54 for C-D type wire coil and from 1.93 to 2.40 for C-type wire coil. While in case of VCTT of same DR and WR , the value of the ratio (Nu_{insert}/Nu_{plane}) ranges from 1.84 to 2.18 for V-cut twisted tape of $TR = 5$, from 1.60 to 1.71 for V-cut twisted tape of $TR = 10$ and from 1.40 to 1.58 for V-cut twisted tape of $TR = 15$. For the same $TR = 10$, the value of the ratio (Nu_{insert}/Nu_{plane}) ranges from 1.70 to 1.90 for V-cut twisted tape of $DR = 0.5$ and $WR = 0.33$ and from 1.55 to 1.77 for V-cut twisted tape of $DR = 0.33$ and $WR = 0.5$.

Fig. 9 shows the variation of friction factor ratio (f_{insert}/f_{plain}) with respect to Reynolds number for different arrangements of enhancers. The friction factor ratio (f_{insert}/f_{plain}) is attained higher with tapered wire coil than V-cut twisted tapes. D-type wire coil shows a maximum value of (f_{insert}/f_{plain}) among all arrangements of enhancers. The value of the

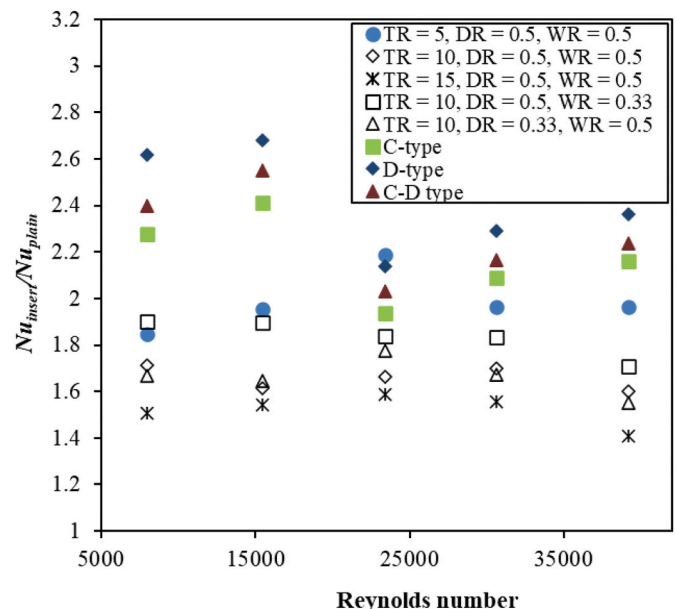


Fig. 8. Variation of Nusselt number enhancement ratio with Reynolds number.

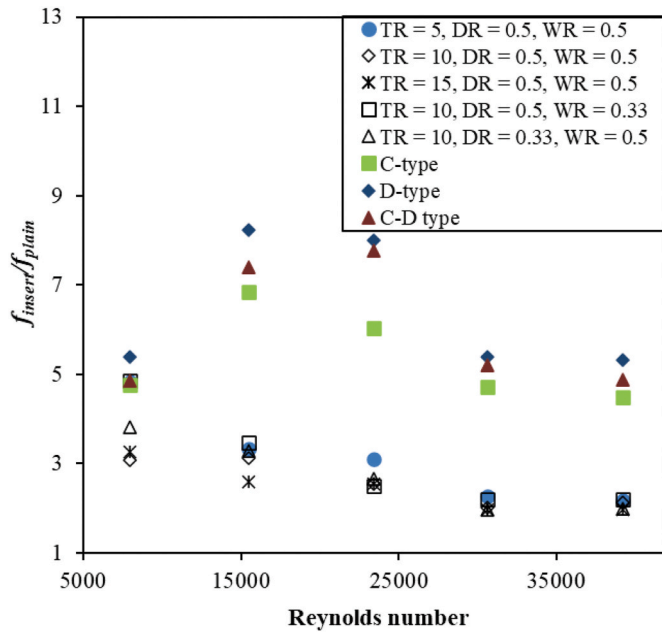


Fig. 9. Variation of friction factor ratio with Reynolds number.

ratio (f_{insert}/f_{plain}) ranges from 5.32 to 8.00 for D-type wire coil, from 4.86 to 7.76 for C-D type wire coil and from 4.48 to 6.83 for C-type wire coil. While in the case of VCTT of same DR and WR, the ratio (f_{insert}/f_{plain}) ranges from 2.18 to 4.82 for V-cut twisted tape of $TR = 5$, from 2.02 to 3.12 for V-cut twisted tape of $TR = 10$ and from 1.95 to 3.26 for V-cut twisted tape of $TR = 15$. For the same $TR = 10$, the ratio (f_{insert}/f_{plain}) ranges from 2.20 to 4.86 for V-cut twisted tape of $DR = 0.5$ and $WR = 0.33$ and from 1.97 to 3.81 for V-cut twisted tape of $DR = 0.33$ and $WR = 0.5$.

3.3. Hydrothermal performance

Fig. 10 shows the effects of different arrangements of enhancers on the performance evaluation criterion (PEC). To evaluate the thermodynamic efficiency of the double pipe heat exchanger, the term PEC has been introduced. The outcomes reveal that the trend of PEC for the

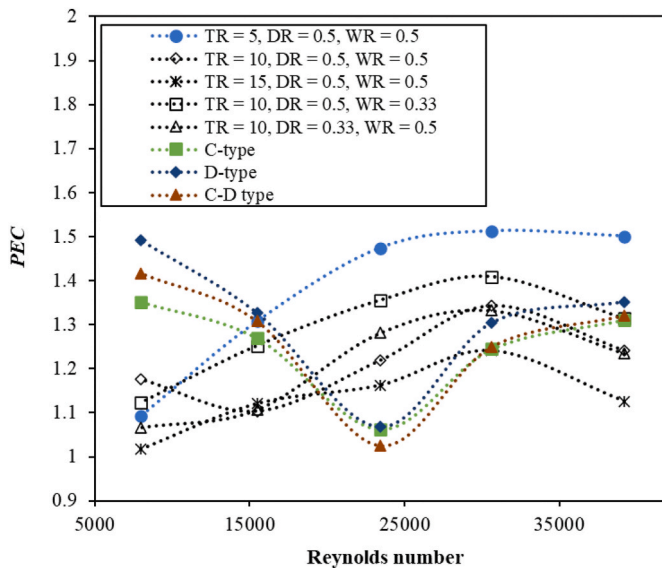


Fig. 10. Variation of PEC with Reynolds number for different enhancer arrangements.

tapered wire coil is different from that for the V-cut twisted tapes and the variation of PEC is not monotonically. While increasing Reynolds number, the PEC increases up to Reynolds number of 30,363 and then decreases for V-cut twisted tapes as the augmentation of Nu is more predominant over the friction factor. While using tapered wire coils, the PEC first decreases up to Reynolds number of 23,415 and then rises with the further increase in Reynolds number. The difference in variational trends of PEC for V-cut twisted tapes and tapered wire coils may be due to their different flow structures as discussed earlier. Meanwhile, the PEC for all arrangements is found greater than one. Among all arrangements of enhancers, the VCTT of $TR = 5$, $DR = 0.5$ and $WR = 0.5$ shows the highest value of PEC, i.e., 1.51 at the Reynolds number of 30,363 and C-D type tapered wire coil shows the minimum value of PEC, i.e., 1.02 at the Reynolds number of 23,415.

The figure of merit (FOM) has been evaluated to characterize the performance of a double pipe heat exchanger as a relative measure of heat transfer enhancement with the penalty of pumping power. Fig. 11 represents the variation of FOM with the nanofluid flow rate for different arrangements of enhancers. The outcomes reveal that the FOM for all arrangements is found greater than one, which can be interpreted that the thermal efficiency of the double tube heat exchanger is increased with the usage of enhancers and nanofluid. The reason is that the augmentation of the heat transfer coefficient is more significant as compared to augmentation in pressure drop. The trend of the tapered wire coil is different from that of the V-cut twisted tapes may be due to their different flow structures, as discussed earlier. As the tapered wire coil inserts offer higher pressure drop, the FOM decreases due to the dominant effect of the higher pumping power. Among all arrangements of enhancers, the VCTT of $TR = 5$, $DR = 0.5$ and $WR = 0.5$ shows the highest value of FOM, i.e., 1.55 at the nanofluid flow rate of 20 lpm and C-D type tapered wire coil shows the minimum value of FOM, i.e., 1.00 at the nanofluid flow rate of 15 lpm, respectively.

The effect of different arrangements of enhancers on the performance index (PI) is illustrated in Fig. 12. From the figure, the value of PI decreases with a rise in the nanofluid flow rate. This is due to the fact that the pumping power rises with a rise in nanofluid flow rate and since PI is the ratio of heat transfer to pumping power, this ratio tends to decrease. The V-cut twisted tapes show a higher value of PI than the tapered wire coil as the augmentation in Δp is less significant in comparison to the enhancement in heat transfer. Among all arrangements of

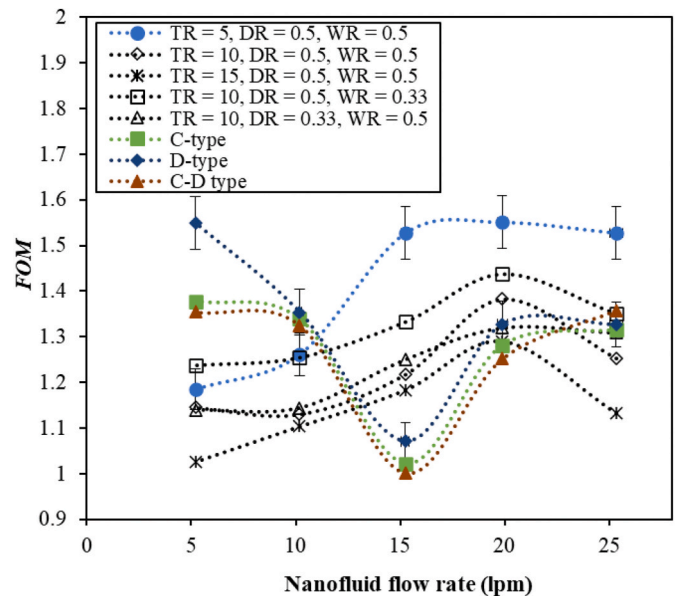


Fig. 11. Variation of FOM with nanofluid flow rate for different enhancer arrangements.

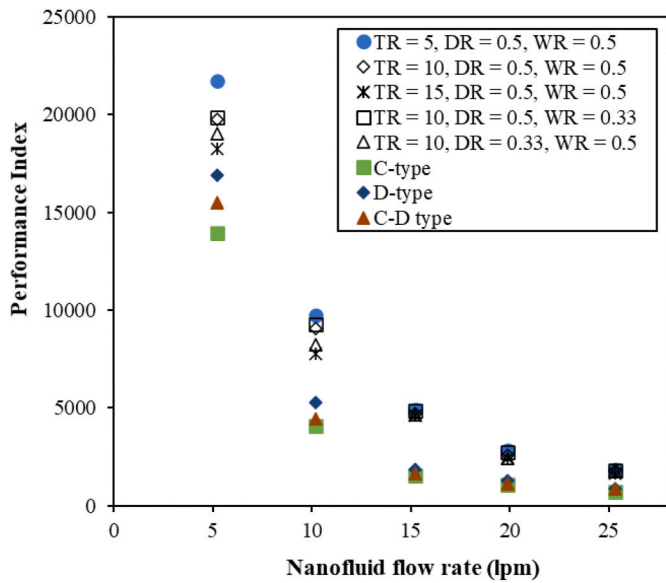


Fig. 12. Variation of PI with nanofluid flow rate for different enhancer arrangements.

enhancers, the VCTT of $TR = 5, DR = 0.5$ and $WR = 0.5$ shows the maximum value of PI , i.e., 21,714 at the nanofluid flow rate of 5 lpm.

3.4. Entropy generation

The thermal entropy generation ($S_{gen,th}$) and frictional entropy generation ($S_{gen,f}$) are depicted in Fig. 13 with respect to Reynolds number for different arrangements of the enhancer. Likely, both $S_{gen,th}$ and $S_{gen,f}$ increases with a rise in Reynolds number. The result reveals that the value of $S_{gen,th}$ with the TWC is lower than with the VCTT as it creates strong mixing of fluids, which in results, improves heat transfer. While the value of $S_{gen,f}$ with TWC is higher than the VCTT as the TWC creates a higher pressure drop in the tube. Since fluid friction irreversibilities is

found very less in comparison to the heat transfer irreversibilities, $S_{gen,tot}$ reduces by the use of TWC in the tube as shown in Fig. 14. D-type wire coil shows the minimum value of the total entropy generation among all arrangements. Also, the outcomes reveal that $S_{gen,tot}$ decreases with decreasing the TR , increase in DR and decrease in WR . Hence, VCTT of $TR = 15, DR = 0.5$ and $WR = 0.5$ shows the maximum value of entropy generation. In comparison to VCTT of $TR = 15, DR = 0.5$ and $WR = 0.5$, the result found a 27.35% average reduction in $S_{gen,tot}$ for D-type wire coil inserts. Moreover, the variation of entropy rises in the tube carrying hybrid nanofluid (ΔS_{nf}) with respect to the Reynolds number for different arrangements of the enhancer is illustrated in Fig. 15. As expected, the outcome exposes that the value of ΔS_{nf} with the TWC is lower than with the VCTT as it provides better heat transfer than that with the

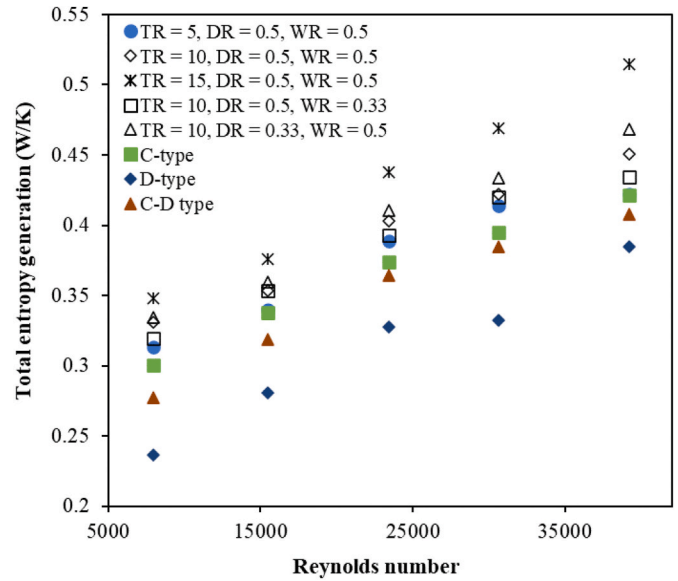


Fig. 14. Variation of total entropy generation with Reynolds number.

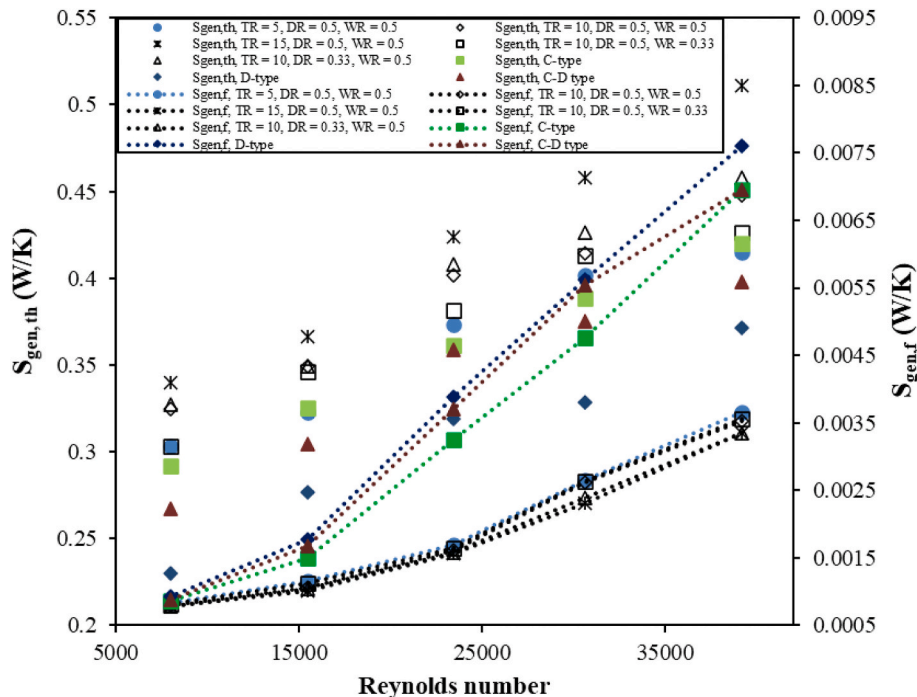


Fig. 13. Variation of thermal entropy generation and frictional entropy generation with Reynolds number.

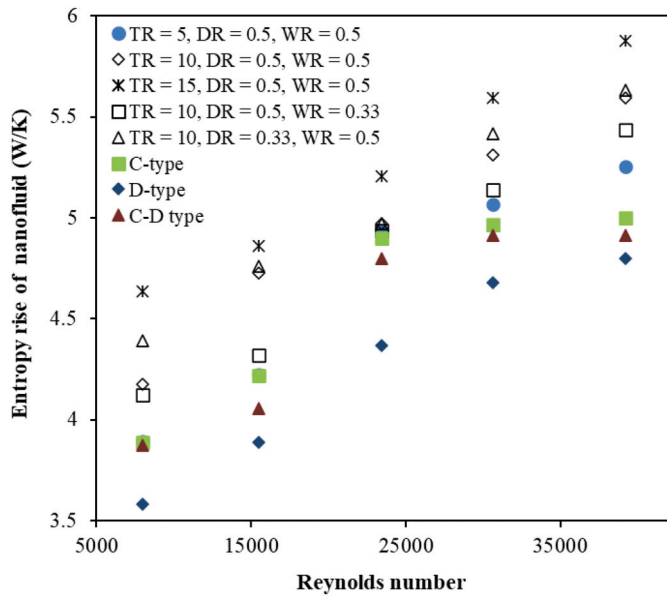


Fig. 15. Variation of entropy rise of nanofluid with Reynolds number.

VCTT. D-type wire coil insert yields a minimum entropy rise of hybrid nanofluid, i.e., 18.70% as compared to that of VCTT of TR = 15, DR = 0.5 and WR = 0.5.

The Bejan number (Be) and entropy generation number (N_s) are depicted in Fig. 16 as a function of Reynolds number for different arrangements of the enhancer. As seen from the figure, Be decreases with an increase in the Reynolds number. The main reason is that the frictional entropy generation increases more rapidly with an increase in the Reynolds number. Also, the value of Be of TWC is higher than that of the VCTT as the $S_{gen,tot}$ of TWC is lower than that of the VCTT. The value of

Be ranges from 0.99 to 0.94 for the range of Reynolds number from 8000 to 40000, which implies that the significance of frictional irreversibility increases with the increase in flow rate. The result reveals that the N_s decreases with increasing Reynolds number due to the domination of the heat capacity rate. The value of N_s ranges from 0.001 to 0.00021 for the range of Reynolds number from 8000 to 40000. D-type TWC yields the lowest N_s due to minimum entropy generation. From the thermodynamic view of point, the lower value of N_s is preferred and this passive technique is advantageous as they augment heat transfer and reduces the irreversibility of the tubular heat exchanger.

3.5. Comparison with other nanofluids and enhancers

The hydrothermal performance of tubular heat exchanger obtained by the present combination (nanofluid and enhancers) is compared with that obtained by other combinations from the previous studies and the comparison of PEC is shown in Table 4. The other nanofluids and enhancers subjected to comparison include CMC-CuO nanofluid with twisted tape of different twist ratio by Bazdidi-Tehrani et al. [20], $Al_2O_3-TiO_2$ nanofluid with V-cut twisted tape of different TR, DR and WR by Singh and Sarkar [23], Al_2O_3-MgO nanofluid with tapered wire coil by Singh and Sarkar [27], Al_2O_3-Cu nanofluid with V-cut twisted tape by Arunachalam and Edwin [38], GnP-Pt/W nanofluid with twin co-twisted tape by Bahiraei et al. [39], TiO_2-SiO_2 nanofluid with wire coil of different pitch ratio by Hamid et al. [40] and Fe_3O_4/W nanofluid with twisted tape with different pitch length by Aghayari et al. [41]. The comparative results reveal that few previous studies [23,40] yield higher PEC values, although all previous studies used higher particle concentration. Hence, it can be concluded that $Al_2O_3+MWCNT$ hybrid nanofluid combined with modified twisted tape and modified wire coil at low nanoparticle volume concentration (0.01%) provides superior PEC value than other combinations of nanofluid and enhancers from the previous studies.

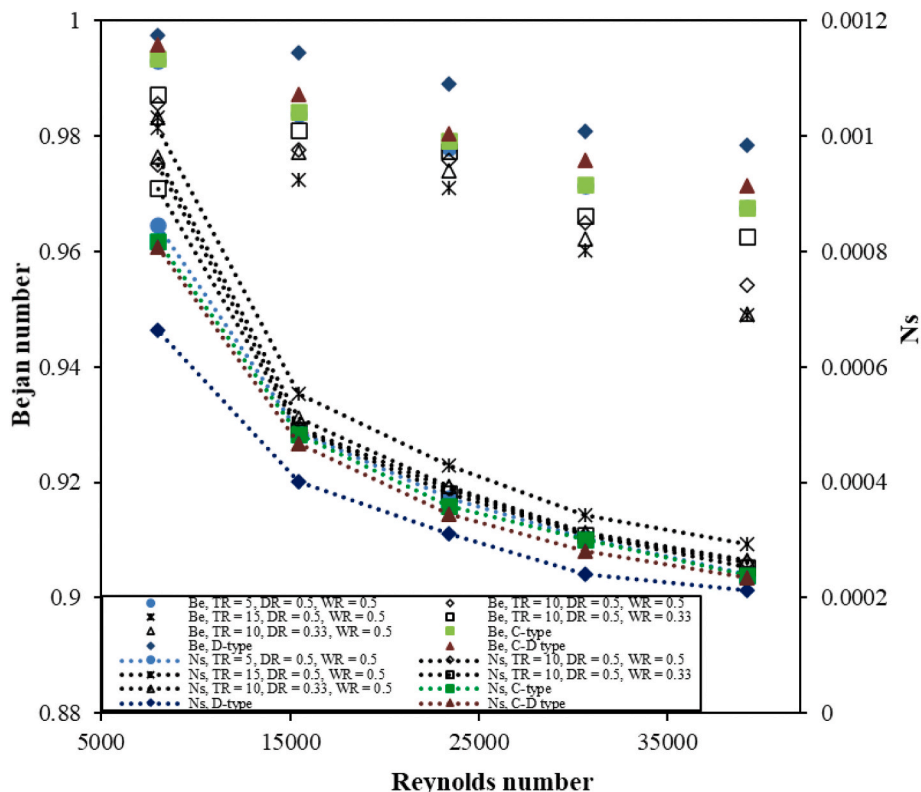


Fig. 16. Variation of Bejan number and entropy generation number with Reynolds number.

Table 4
Comparison of presently obtained PEC values with previous studies.

Authors	Nanofluids	Enhancer	Conditions	PEC value
Present Study	Al ₂ O ₃ +MWCNT (Vol % = 0.01)	V-cut TT and TWC	8000 < Re < 40000	1.01–1.51
Bazdidi-Tehrani et al. [20]	CMC-CuO (vol% = 0.1–1.5)	TT, TR = 5, 10, 15 and 83	2500 < Re < 10000	1.18–1.62
Singh and Sarkar [23]	Al ₂ O ₃ -TiO ₂ (Vol % = 0.1)	VTT, TR = 5–15, Pe = 5–7.5 mm, w = 5–7.5 mm	9000 < Re < 40000	1.09–2.51
Singh and Sarkar [27]	Al ₂ O ₃ -MgO (Vol % = 0.1)	TWC, C-type, D type and C-D type TWC	9000 < Re < 40000	1.06–1.69
Arunachalam and Edwin [38]	Al ₂ O ₃ -Cu (vol% = 0.1–0.4)	VTT, Pe = 8 mm, w = 10 mm	2580 < Pe < 11780	1.01–1.05
Bahiraie et al. [39]	GnP-Pt/W (Vol % = 0.02–0.1)	Twin Co-TT, TR = 2.5, 3 and 3.5	5000 < Re < 20000	1.01–1.28
Hamid et al. [40]	TiO ₂ -SiO ₂ (Vol % = 0.5–3)	Wire coil P/D = 0.83–4.17	2300 < Re < 12000	1.3 to 2.06
Aghayari et al. [41]	Fe ₃ O ₄ /W (Vol % = 0.08–0.1)	TT, TR = 2.5–5.2	5000 < Re < 28500	1.00–1.62

4. Conclusions

In the current study, the experimental outcomes of heat transfer, pressure drop and hydrothermal performances of double tube heat exchanger using Al₂O₃+MWCNT hybrid nanofluid with various enhancers (VCTT and TWC) are reported and compared. The following outcomes are provided from the present study:

- The heat transfer coefficient increases with reducing twist ratio, increase in *DR* and decrease in *WR* in the case of V-cut twisted tapes. D-type wire coil exhibits better heat transfer performance than other tapered wire coils.
- Pressure drop is higher for tapered wire coil as compared to V-cut twisted tape. D-type wire coil shows higher values than other arrangements. Pressure drop rises with reducing twist ratio, raising *DR* and reducing *WR*.
- For all arrangements, the *PEC* and *FOM* are found greater than one. The VCTT of *TR* = 5, *DR* = 0.5 and *WR* = 0.5 shows the maximum values of *PEC* and *FOM*; whereas C-D type tapered wire coil shows the minimum value of *PEC* and *FOM*.
- *PI* decreases with a rise in the nanofluid flow rate. The VCTT shows a higher value of *PI* than the TWC as the augmentation in pressure drop is less significant in comparison to the augmentation in heat transfer.
- D-type wire coil shows a minimum entropy generation among all arrangements. In comparison to VCTT of *TR* = 15, *DR* = 0.5 and *WR* = 0.5, the D-type wire coil yields an average 27.35% reduction in total entropy generation. Frictional entropy generation is negligibly small as compared to thermal entropy generation.

Declaration of competing interest

The authors declare that they have no known competing financial interests or personal relationships that could have appeared to influence the work reported in this paper.

Data availability

Data will be made available on request.

References

- [1] C.K. Mangrulkar, A.S. Dhoble, S. Chamoli, A. Gupta, V.B. Gawande, Recent advancement in heat transfer and fluid flow characteristics in cross flow heat exchangers, *Renew. Sustain. Energy Rev.* 113 (2019) 109220.
- [2] L. Wang, B. Sundén, Performance comparison of some tube inserts, *Int. Commun. Heat Mass Tran.* 29 (2002) 45–56.
- [3] S. Eiamsa-Ard, V. Kongkaiptaiboon, P. Promvongse, Thermal performance assessment of turbulent tube flow through wire coil turbulators, *Heat Tran. Eng.* 32 (2011) 957–967.
- [4] H. Karakaya, A. Durmus, Heat transfer and exergy loss in conical spring turbulators, *Int. J. Heat Mass Tran.* 60 (2013) 756–762.
- [5] S. Bhattacharyya, H. Chattopadhyay, S. Bandyopadhyay, Numerical study on heat transfer enhancement through a circular duct fitted with centre-trimmed twisted tape, *Int. J. Heat Technol.* 34 (2016) 401–406.
- [6] S. Bhattacharyya, H. Chattopadhyay, A.C. Benim, Simulation of heat transfer enhancement in tube flow with twisted tape insert, *Prog. Comput. Fluid Dynam.* Int. J. 17 (2017) 193–197.
- [7] S. Bhattacharyya, H. Chattopadhyay, A.C. Benim, Computational investigation of heat transfer enhancement by alternating inclined ribs in tubular heat exchanger, *Prog. Comput. Fluid Dynam.* Int. J. 17 (2017) 390–396.
- [8] S. Bhattacharyya, H. Chattopadhyay, A. Guin, A.C. Benim, Investigation of inclined turbulators for heat transfer enhancement in a solar air heater, *Heat Tran. Eng.* 40 (2018) 1451–1460.
- [9] S. Bhattacharyya, A.C. Benim, H. Chattopadhyay, A. Banerjee, Experimental investigation of heat transfer performance of corrugated tube with spring tape inserts, *Exp. Heat Tran.* 32 (2019) 411–425.
- [10] M.E. Nakhchi, M. Hatami, M. Rahmati, Experimental investigation of heat transfer enhancement of a heat exchanger tube equipped with double-cut twisted tapes, *Appl. Therm. Eng.* 180 (2020) 115863.
- [11] S. Chamoli, R. Lu, P. Yu, Thermal characteristic of a turbulent flow through a circular tube fitted with perforated vortex generator inserts, *Appl. Therm. Eng.* 121 (2017) 1117–1134.
- [12] S. Chamoli, R. Lu, J. Xie, P. Yu, Numerical study on flow structure and heat transfer in a circular tube integrated with novel anchor shaped inserts, *Appl. Therm. Eng.* 135 (2018) 304–324.
- [13] K. Ponweiser, W. Linzer, M. Malinovec, Performance comparison between wire coil and twisted tape inserts, *J. Enhanc. Heat Transf.* 11 (2004) 359–370.
- [14] M. Khoshvaght-Aliabadi, S. Davoudi, M.H. Dibaei, Performance of agitated-vessel U tube heat exchanger using spiky twisted tapes and water based metallic nanofluids, *Chem. Eng. Res. Des.* 133 (2018) 26–39.
- [15] E.F. Akyurek, K. Gelis, B. Sahin, E. Manay, Experimental analysis for heat transfer of nanofluid with wire coil turbulators in a concentric tube heat exchanger, *Results Phys* 9 (2018) 376–389.
- [16] V.V. Rao, M.C. Reddy, Experimental investigation of heat transfer coefficient and friction factor of ethylene glycol water based TiO₂ nanofluid in double pipe heat exchanger with and without helical coil inserts, *Int. Commun. Heat Mass Tran.* 50 (2014) 68–76.
- [17] M. Mirzaei, A. Azimi, Heat transfer and pressure drop characteristics of graphene oxide/water nanofluid in a circular tube fitted with wire coil insert, *Exp. Heat Tran.* 29 (2016) 173–187.
- [18] S. Eiamsa-ard, K. Wongcharee, K. Kunrarak, M. Kumar, V. Chuwattabakul, Heat transfer enhancement of TiO₂-water nanofluid flow in dimpled tube with twisted tape insert, *Heat Mass Tran.* 55 (2019) 2987–3001.
- [19] W. He, D. Toghraie, A. Lotfipour, F. Pourfatah, A. Karimipour, M. Afrand, Effect of twisted-tape inserts and nanofluid on flow field and heat transfer characteristics in a tube, *Int. Commun. Heat Mass Tran.* 110 (2020) 104440.
- [20] F. Bazdidi-Tehrani, S.M. Khanmohamadi, S.I. Vasefi, Evaluation of turbulent forced convection of non-Newtonian aqueous solution of CMC/CuO nanofluid in a tube with twisted tape inserts, *Adv. Powder Technol.* 31 (2020) 1100–1113.
- [21] M.T. Naik, S.S. Fahad, L.S. Sundar, M.K. Singh, Comparative study on thermal performance of twisted tape and wire coil inserts in turbulent flow using CuO/water nanofluid, *Exp. Therm. Fluid Sci.* 57 (2014) 65–76.
- [22] M.A. Akhavan-Behabadi, M. Shahidi, M.R. Aligodarz, Mohammad Ghazvini, Experimental investigation on thermo-physical properties and overall performance of MWCNT-water nanofluid flow inside horizontal coiled wire inserted tubes, *Heat Mass Tran.* 53 (2017) 291–304.
- [23] S.K. Singh, J. Sarkar, Improving hydrothermal performance of double-tube heat exchanger with modified twisted tape inserts using hybrid nanofluid, *J. Therm. Anal. Calorim.* (2020), <https://doi.org/10.1007/s10973-020-09380-w>.
- [24] H. Maddah, R. Aghayari, M. Mirzaei, M.H. Ahmadi, M. Sadeghzadeh, A. J. Chamkha, Factorial experimental design for the thermal performance of a double pipe heat exchanger using Al₂O₃-TiO₂ hybrid nanofluid, *Int. Commun. Heat Mass Tran.* 97 (2018) 92–102.
- [25] S.K. Singh, J. Sarkar, Experimental hydrothermal characteristics of concentric tube heat exchanger with V-cut twisted tape turbulator using PCM dispersed mono/hybrid nanofluids, *Exp. Heat Tran.* (2020), <https://doi.org/10.1080/08916152.2020.1772412>.
- [26] M. Bahiraie, N. Mazaheri, F. Aliee, Second law analysis of a hybrid nanofluid in tubes equipped with double twisted tape inserts, *Powder Technol.* 345 (2019) 692–703.
- [27] S.K. Singh, J. Sarkar, Improving hydrothermal performance of hybrid nanofluid in double tube heat exchanger using tapered wire coil turbulator, *Adv. Powder Technol.* 31 (2020) 2092–2100.

- [28] Z. Li, M.M. Sarafraz, A. Mazinani, T. Hayat, H. Alsulami, M. Goodarzi, Pool boiling heat transfer to CuO-H₂O nanofluid on finned surfaces, *Int. J. Heat Mass Tran.* 156 (2020) 119780.
- [29] Z. Li, A. Mazinani, T. Hayat, A.A.A.A. Al-Rashed, H. Alsulami, M. Goodarzi, M. M. Sarafraz, Transient pool boiling and particulate deposition of copper oxide nano-suspensions, *Int. J. Heat Mass Tran.* 155 (2020) 119743.
- [30] V. Kumar, J. Sarkar, Experimental hydrothermal characteristics of minichannel heat sink using various types of hybrid nanofluids, *Adv. Powder Technol.* 31 (2020) 621–631.
- [31] B.P. Singh, R. Menchavez, C. Takai, M. Fuji, M. Takahashi, Stability of dispersions of colloidal alumina particles in aqueous suspensions, *J. Colloid Interface Sci.* 291 (2005) 181–186.
- [32] B.P. Singh, S. Nayak, S. Samal, S. Bhattacharjee, L. Besra, Characterization and dispersion of multiwalled carbon nanotubes (MWCNTs) in aqueous suspensions: surface chemistry aspects, *J. Dispersion Sci. Technol.* 33 (2012) 1021–1029.
- [33] J. Dirker, J.P. Meyer, Heat transfer coefficients in concentric annuli, *J. Heat Tran.* 124 (2002) 1200–1202.
- [34] S.J. Kline, F.A. McClintock, Describing uncertainties in single-sample experiments, *Mech. Eng.* 75 (1953) 3–8.
- [35] F.P. Incropera, P.D. DeWitt, T.L. Bergman, A.S. Lavine, *Fundamentals of Heat and Mass Transfer*, John-Wiley & Sons, USA, 2006.
- [36] K. Nanan, C. Thianpong, P. Promvong, S. Eiamsa-ard, Investigation of heat transfer enhancement by perforated helical twisted-tapes, *Int. Commun. Heat Mass Tran.* 52 (2014) 106–112.
- [37] B. Kumar, G.P. Srivastava, M. Kumar, A.K. Patil, A review of heat transfer and fluid flow mechanism in heat exchanger tube with inserts, *Chem. Eng. Process* 123 (2018) 126–137.
- [38] U. Arunachalam, M. Edwin, Experimental studies on laminar flow heat transfer in nanofluids flowing through a straight circular tube with and without V-cut twisted tape insert, *Heat Mass Tran.* 54 (2018) 673–683.
- [39] M. Bahiraei, N. Mazaheri, S.M. Hassanzamani, Efficacy of a new graphene–platinum nanofluid in tubes fitted with single and twin twisted tapes regarding counter and co-swirling flows for efficient use of energy, *Int. J. Mech. Sci.* 150 (2018) 290–303.
- [40] K.A. Hamid, W.H. Azmi, R. Mamat, K.V. Sharma, Heat transfer performance of TiO₂–SiO₂ nanofluids in a tube with wire coil Inserts, *Appl. Therm. Eng.* 152 (2019) 275–286.
- [41] R. Aghayari, H. Maddah, S.M. Pourkiaei, M.H. Ahmadi, L. Chen, M. Ghazvini, Theoretical and experimental studies of heat transfer in a double-pipe heat exchanger equipped with twisted tape and nanofluid, *Eur. Phys. J. Plus* 135 (2020) 252.